Perspectives on: Local calcium signaling

Recording single-channel activity of inositol trisphosphate receptors in intact cells with a microscope, not a patch clamp

Ian Parker[1,2] and Ian F. Smith[1]

[1]Department of Neurobiology and Behavior, and [2]Department of Physiology and Biophysics, University of California, Irvine, Irvine, CA 92697

The Journal of General Physiology

Introduction

Cytosolic Ca^{2+} plays a central role as a universal intracellular messenger, controlling many aspects of physiology such as gene expression, electrical excitability, secretion, and synaptic plasticity in virtually all cell types (Berridge et al., 2000). The rich diversity in information encoded by Ca^{2+} arises through the mechanisms by which Ca^{2+} signals are generated and transmitted to act over very different spatial and temporal scales. For example, locally high [Ca^{2+}] can trigger neurotransmitter release within microseconds of Ca^{2+} entry through voltage-gated channels closely apposed to active release zones (Neher, 1998), whereas globally propagating Ca^{2+} waves with periods measured in minutes regulate gene expression (Dolmetsch et al., 1998; Bootman et al., 2001). Resting [Ca^{2+}] in the cytosol is maintained at low nanomolar levels, and Ca^{2+} signals are generated by Ca^{2+} ions entering the cytosol both across the plasma membrane through voltage- and ligand-gated channels and store-operated calcium channels, and by liberation of Ca^{2+} from intracellular stores such as the ER through Ca^{2+} release channels. The inositol trisphosphate (IP_3) receptor (IP_3R) is one of the two major Ca^{2+} release channels located on the ER, and it is the focus of our discussion.

The spatiotemporal patterning and transmission of Ca^{2+} signals involve the inherent properties of the Ca^{2+} channels themselves, their spatial organization, and how these channels interact via diffusion of Ca^{2+} both with themselves and with effector proteins. The IP_3R channel exhibits particular complexity because its opening requires binding of the second messenger IP_3 together with Ca^{2+} to receptor sites on the cytosolic face. Gating by Ca^{2+} is biphasic, such that small elevations of cytosolic Ca^{2+} induce channel opening, whereas larger elevations cause inactivation (Bezprozvanny et al., 1991; Foskett et al., 2007). Thus, there exists the potential for both positive and negative feedback loops, whereby Ca^{2+} liberated through one channel may modulate its own opening and that of neighboring channels. Channel–channel interactions are delimited by the spatial arrangement of channels, and IP_3Rs are organized into tight clusters on the ER membrane. This leads to a hierarchy of calcium signals of differing magnitudes (Lipp and Niggli, 1996a; Parker et al., 1996). "Fundamental" signals (Ca^{2+} blips) represent Ca^{2+} flux through individual IP_3R channels (Parker and Yao, 1991, 1996; Thomas et al., 2000; Rose et al., 2006); "elementary" Ca^{2+} transients (Ca^{2+} puffs) are generated by the openings of multiple IP_3R within a cluster, orchestrated by Ca^{2+}-induced Ca^{2+} release (CICR); and propagating global waves of Ca^{2+} result from progressive recruitment across multiple clusters by successive cycles of Ca^{2+} diffusion and CICR (Thorn et al., 1993; Yao et al., 1995; Berridge, 1997; Bootman et al., 1997a,b). The transitions between blips, puffs, and global Ca^{2+} waves are determined by factors such as stimulus strength ([IP_3] and cytosolic [Ca^{2+}]) (Callamaras et al., 1998a), the density of IP_3R within a cluster (Shuai et al., 2006), the spacing between clusters (Callamaras et al., 1998b), and the action of mobile and immobile cytosolic Ca^{2+} buffers to affect the diffusion of Ca^{2+} ions (Dargan and Parker, 2003; Dargan et al., 2004).

The goal of our laboratory has been to use ever-improving imaging modalities to better resolve the hierarchical components and underlying mechanisms of IP_3-mediated Ca^{2+} signaling in intact cells. This has involved a journey from using wide-field fluorescence microscopy for imaging of global Ca^{2+} transients, to applying total internal reflection microscopy to resolve the activity and localization of single IP_3R channels. Here, we review different techniques that have contributed to an understanding of how IP_3Rs are organized and focus on our recent work taking functional imaging studies down to the single-molecule level.

Correspondence to Ian F. Smith: ismith@uci.edu

Abbreviations used in this paper: CICR, Ca^{2+}-induced Ca^{2+} release; IP_3, inositol trisphosphate; IP_3R, IP_3 receptor; TIRF, total internal reflection fluorescence.

The Rockefeller University Press $30.00
J. Gen. Physiol. Vol. 136 No. 2 119–127
www.jgp.org/cgi/doi/10.1085/jgp.200910390

Electrophysiology versus optophysiology

The gold standard for studying single ion channels is the electrophysiological patch clamp, which monitors current flow through single channels with pico ampere and millisecond resolution (Neher and Sakmann, 1976; Hamill et al., 1981). This technique is readily applied to plasmalemmal channels, but intracellular channels such as the IP_3R are largely out of reach of the patch pipette within their native environment in intact cells. Electrophysiological studies have, therefore, used reduced systems, such as reconstitution of IP_3Rs into lipid bilayers (Ehrlich and Watras, 1988; Bezprozvanny et al., 1991) and patch clamping of IP_3Rs on the membrane of excised nuclei (Mak and Foskett, 1994). Both of these approaches allow for high resolution recording of single-channel activity under tightly controlled ionic and electrical conditions. Nevertheless, they suffer from significant drawbacks, including disruption of the spatial organization of IP_3Rs, possible loss of the accessory proteins and modulatory molecules, and disruption of channel–channel interactions mediated by CICR and Ca^{2+} diffusion.

There has thus been a long-standing interest in the development of minimally invasive optical imaging techniques to provide complimentary information about IP_3R functioning within intact cells. These approaches have largely been based on the small molecule indicator dyes originally developed by Roger Tsien and, in particular, on the visible wavelength dyes such as fluo-4, which, although they do not allow for true ratiometric measurements, provide bright fluorescence signals with wide dynamic range (Grynkiewicz et al., 1985; Minta et al., 1989; Gee et al., 2000). Because of the very low resting cytosolic concentration of free Ca^{2+}, the opening of even a single Ca^{2+}-permeable channel generates an enormous increase in Ca^{2+} concentration in the immediate vicinity of the channel pore: from ~50 nM to tens or even hundreds of μM (Shuai and Parker, 2005). Moreover, optical measurements have, in theory at least, an advantage over electrophysiological recording in that whereas a single Ca^{2+} ion moving through a channel contributes just two positive charges to the current, a Ca^{2+}-bound fluorophore molecule can be excited to emit many thousands of photons. In practice, however, imaging technology has only recently improved to the point where single-channel activity can reliably be visualized with millisecond resolution. Along the way, advances in technology have been responsible for progressively revealing the hierarchy of IP_3-mediated Ca^{2+} signaling, from waves to elementary puffs to fundamental blips.

Cellular Ca^{2+} imaging: from global waves to fundamental blips

The *Xenopus* oocyte has long been a favored model cell to study IP_3-mediated Ca^{2+} signaling, owing to its large size that facilitates microinjection and its lack of ER Ca^{2+} release channels other than IP_3Rs (i.e., RYRs and cADP-ribose receptors) (Parys et al., 1992). Early experiments using confocal microscopy at a slow frame rate of 1 s^{-1} revealed propagating Ca^{2+} waves evoked by IP_3-mobilizing agonists, which often self-organized into beautiful and complex spiral patterns (Lechleiter et al., 1991). Contemporaneously, wide-field fluorescence imaging using a camera at faster frame rate (30 s^{-1}), in conjunction with flash photolysis of caged IP_3 to permit precise regulation of cytosolic [IP_3], led to the discovery of transient, localized puffs (Parker and Yao, 1991; Yao and Parker, 1994; Yao et al., 1995), the first member of an ever-growing bestiary of elementary Ca^{2+} signals, including the analogous sparks generated by RYR in cardiac muscle (Cheng et al., 1993; Cheng and Lederer, 2008). More detailed analyses of puffs were then accomplished using video-rate (30 s^{-1}) frame-scanning confocal microscopy (Yao et al., 1995) and by line scan confocal imaging, whereby temporal resolution is improved to as much as 1,000 scans s^{-1} at the expense of capturing information in only one spatial dimension. Puffs in both oocytes (Yao et al., 1995) and cultured mammalian cells (Thorn et al., 1993; Bootman et al., 1997a; Thomas et al., 2000) displayed apparently monotonic rising phases lasting tens of milliseconds while Ca^{2+} was liberated, followed by a slower decay as the Ca^{2+} microdomain at the puff site dissipated after channel closure (Thorn et al., 1993; Yao et al., 1995; Bootman et al., 1997a). Estimates of the amount of Ca^{2+} released during puffs already suggested that they must involve the opening of more than a single IP_3R channel, and this view was reinforced by the resolution of yet smaller events, Ca^{2+} blips, that were first detected using a point confocal microscope (Parker and Yao, 1996) and were subsequently spatially resolved in HeLa cells by line scan imaging (Bootman et al., 1997b). Blips were interpreted as fundamental events, arising from the openings of individual IP_3R, and in parallel, the discovery of analogous Ca^{2+} quarks (Lipp and Niggli, 1996b) suggested that these are the fundamental RYR channel events from which sparks are constituted. However, although these and other reports describe specific instances of single IP_3R channel fluorescence signals (Parker and Yao, 1996; Bootman et al., 1997b; Rose et al., 2006), none of these imaging modalities provided the spatiotemporal resolution necessary for detailed quantitative studies nor to dissect the contributions of individual channels during puffs.

Issues in optical resolution of single-channel activity

What then is required to image single-channel Ca^{2+} signals with good fidelity? The opening of a single Ca^{2+}-permeable channel or tightly grouped cluster of channels establishes an extremely steep gradient of cytosolic [Ca^{2+}]. Modeling studies show that the concentration may reach hundreds of μM at nanometer

distances from the channel pore, yet fall to only tens of nM above the resting level at distances of a few μm (Shuai and Parker, 2005). Moreover, there are steep temporal gradients. The Ca^{2+} concentration near the pore rises and falls within microseconds of channel opening and closing, whereas concentrations a few μm away change over tens or hundreds of milliseconds. Ideally, we would like to be able to monitor the local [Ca^{2+}] in the immediate vicinity of the channel pore with submillisecond temporal resolution. The genetic targeting of fast indicators to channel proteins holds promise (Giepmans et al., 2006), but at present, the best results have been achieved using soluble small molecule dyes such as fluo-4. Given that both Ca^{2+} ions and, to a greater extent, Ca^{2+}-bound dye molecules are motile in the cytosol, the fluorescence signal arising from a single-channel opening becomes spatially and temporally blurred by the combined effects of diffusion and the kinetics of Ca^{2+} binding and unbinding to the indicator. Imaging the fluorescence then introduces yet a further blurring by the diffraction-limited point-spread function of the microscope. In terms of instrumentation, the temporal resolution and signal amplitude can be improved by reducing the cytosolic volume from which fluorescence signals are monitored. But this involves a compromise because smaller volumes encompass progressively fewer Ca^{2+}-bound dye molecules, so that statistical fluctuations ("molecular shot noise") increasingly degrade the signal/noise ratio. Simulations suggest that sampling volumes of the order of a few tens of atto liters ($10–50 \times 10^{-18}$ l) would be optimal (Shuai and Parker, 2005). In parallel, cells can be loaded with a nonfluorescent Ca^{2+} chelator with slower binding kinetics than the indicator dye, such as EGTA, into the cytosol. This competes with the indicator for Ca^{2+} and both speeds the decay of fluorescence after channel closure and "sharpens" the spatial profile of the fluorescence signal (Shuai and Parker, 2005; Zeller et al., 2009). Again, a compromise is required because too much chelator will unacceptably reduce the amplitude of the fluorescence signal.

Technologies to resolve elementary and fundamental Ca^{2+} signals

As noted above, the key to obtaining good optical single-channel Ca^{2+} records is to monitor fluorescence from a very small cytosolic volume and to accomplish this rapidly enough to resolve channel gating on a millisecond timescale. A recurring theme has been that both engineering and fundamental limitations have necessitated a trade-off between either spatial or temporal resolution. Wide-field fluorescence microscopy can be used with cameras having fast frame rates (hundreds of frames s^{-1}) (Zou et al., 2004), but it typically provides little or no depth (z-axis) discrimination; although schemes using fast z-axis stepping (Kirber et al., 2001) or multiple cameras with offset focal planes (Demuro and Parker, 2008) can mitigate that limitation. Confocal and multiphoton microscopy achieve a tightly delimited 3-D point-spread function (typical dimensions of ∼300 nm laterally and 800 nm axially with objectives of high numerical aperture), with sub-femtoliter volume. However, these are inherently point-scanning systems, wherein mechanical constraints may limit the speed at which the laser spot can be scanned. Although technologies such as resonant scanning mirrors (Nguyen et al., 2001) and accousto-optic deflectors provide faster scans (Lechleiter et al., 2002), they have their own specific drawbacks, and all approaches are ultimately limited by the need to detect sufficient fluorescence photons. At the shot-noise limit, the signal/noise ratio varies as the square root of light intensity, so the image quality degrades with increasing scan rates and pixel resolution as the dwell-time at each pixel becomes shorter.

A popular compromise for imaging elementary Ca^{2+} events has been the use of confocal line scan imaging, in which the confocal spot is repeatedly scanned along a single line to derive an image representing the temporal evolution of Ca^{2+} signals in one spatial dimension. Advantages include high temporal resolution and relatively long pixel dwell times because only a small number of pixels are scanned along the single line, as well as the ability to present results as an individual image with Ca^{2+} levels encoded by color and/or height representation. Drawbacks include the restriction of sampling to a single line through a cell and, more seriously, the difficulty of ascertaining whether a signal is in focus or arose from a site distant from the scan line. Nonfocal fluorescence signals will be of smaller amplitude and display slowed kinetics, complicating interpretation of experimental results (Izu et al., 1998), with the exception of instances such as a channel trapped at the tip of a patch pipette where the location is precisely known and can be aligned with the scan line (Wang et al., 2001).

Total internal reflection fluorescence (TIRF) microscopy: a good way to image Ca^{2+} signals near the plasma membrane

TIRF microscopy has more recently been applied to image local Ca^{2+} signals, and it combines the advantages of fast camera-based imaging together with an optical sectioning effect (z-axis resolution) even finer than confocal microscopy (Demuro and Parker, 2004, 2005; Navedo et al., 2006). TIRF works by directing excitation light through a glass substrate toward an aqueous specimen at a sufficiently shallow angle so that total internal reflection occurs due to the refractive index decrease at the glass–water interface. However, a very thin electromagnetic field (evanescent wave) is created in the liquid with the same wavelength as the incident light and decays exponentially with distance from the interface (typically over one or a few hundred nm). Because this field is able to excite fluorophores near the interface

while avoiding excitation further into the aqueous phase, it provides an "optical sectioning" effect similar to, but even narrower, than that achieved by a confocal microscope (Axelrod, 2003). Although the idea of TIRF microscopy is old, its biological utility has expanded greatly in the last few years after the commercial introduction of specialized oil-immersion objective lenses with very high numerical aperture (1.45 or greater). These allow the excitation light to be directed to the specimen at the necessarily shallow angle through the very edge of the lens while collecting emitted fluorescence back through the same objective. In conjunction with developments in low noise electron-multiplied CCD cameras, this enables two-dimensional records to be acquired at high frame rates (1,000 s^{-1} or better with pixel binning) and good signal/noise ratio. Measurements from small (sub-μm) regions of interest can then be used to monitor fluorescence from attoliter cytosolic volumes centered on active Ca^{2+} release sites. The main disadvantage of TIRF microscopy is that it can image only in the immediate vicinity of the cover glass and is thus applicable exclusively to signals arising close to the cell membrane. TIRF has thus been used primarily to study Ca^{2+} flux through plasmalemmal channels (Demuro and Parker, 2004, 2005; Navedo et al., 2006), although it is also applicable to intracellular Ca^{2+} release channels that lie close to the membrane (Smith and Parker, 2009; Smith et al., 2009a,b; Wiltgen et al., 2010).

How should we interpret local Ca^{2+} fluorescence signals? Fluorescence signals originating from single or tightly clustered Ca^{2+} channels provide only a distorted impression of the underlying Ca^{2+} gradient and are heavily smoothed in both space and time. Thus, it is worth emphasizing the complications that arise when attempting to interpret and quantify local fluorescence signals, especially because the interpretation depends strongly upon the method used to acquire the images. We can consider two extreme cases.

In the first (approximated by wide-field imaging), fluorescence is collected from a large volume around a localized Ca^{2+} source, such as a single channel or tight cluster of channels (Zou et al., 2004). The fluorescence signal then represents an integral of Ca^{2+} release and, neglecting possible indicator saturation near the channel, is not affected by diffusion of Ca^{2+} ions or Ca^{2+}-bound indicator because little escapes outside the large imaging volume. Given that Ca^{2+} sequestration mechanisms (pumps and transporters) are slow on the timescale of elementary and fundamental events, the slope of the rising phase of the fluorescence signal provides a measure of Ca^{2+} flux (current), and the peak signal provides a measure of the total amount (moles) of Ca^{2+} entering the cytosol. The latter measure of "signal mass" was first applied by considering line scan records as a diametric slice through a 3-D volume (Sun et al., 1998; Hollingworth et al., 2001), and it was subsequently applied to wide-field images (Zou et al., 2004). Although in principle the rising phase reflects Ca^{2+} flux, differentiation of the fluorescence record usually results in a signal that is too noisy to provide useful information about channel gating kinetics.

The second case is when fluorescence is monitored from an exceedingly small volume around the channel pore. Ideally, this would then provide a signal directly analogous to a patch clamp record; i.e., the fluorescence amplitude would be directly and linearly proportional to instantaneous Ca^{2+} flux (current). TIRF microscopy approaches this condition, but only approximately, as a result of factors including indicator binding kinetics and diffusion together with the finite imaging volume. Nevertheless, single-channel records obtained using TIRF as an "optical patch clamp" closely resemble electrophysiological recordings and can track channel gating with a resolution of ∼2 ms (Demuro and Parker, 2005). Calibration of the fluorescence amplitude in terms of underlying Ca^{2+} current is more problematic, but an in situ estimate may be obtained by measuring fluorescence signals under conditions that correspond to a known Ca^{2+} current as measured by parallel patch clamp recording.

Local measurements of elementary and fundamental Ca^{2+} signals obtained by confocal microscopy lie intermediate between the above two extreme situations. That is to say, the fluorescence can be considered as a "leaky integral," reflecting a balance between Ca^{2+} efflux into the cytosol and its subsequent diffusion out of the region of interest from which fluorescence is measured. The rising phase thus approximates the duration of Ca^{2+} flux (i.e., when channels are open), whereas the falling phase largely reflects diffusive spread of Ca^{2+} ions in the cytosol. The peak amplitude may be affected both by the magnitude and the duration of Ca^{2+} flux. We argue in particular that it is not valid to apply steady-state calibrations of indicator fluorescence to estimate the peak local cytosolic free Ca^{2+} concentrations during elementary events, given that the fluorescence is a highly blurred reflection of the underlying steep Ca^{2+} concentration gradient. For the same reason, the spatial extent of local fluorescence signals does not directly report the spatial spread of free Ca^{2+} or the distribution of Ca^{2+} channels within a small cluster, although this information can be applied in simulation and computational studies to estimate these parameters (Shuai and Parker, 2005; Ventura et al., 2005).

Applications of TIRF microscopy for imaging elementary and fundamental Ca^{2+} signals in mammalian cells. By imaging the local fluorescence changes with a high speed (500 frames s^{-1}), high sensitivity (back-illuminated electron-multiplied CCD) camera, we have achieved

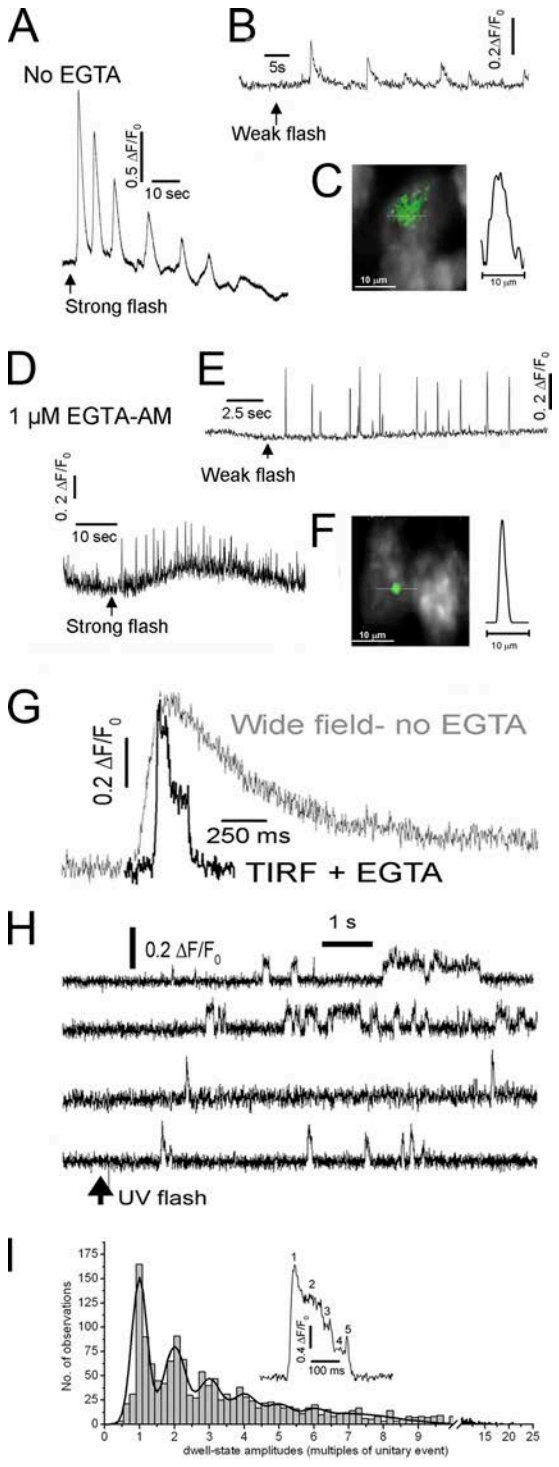

Figure 1. Dissecting the hierarchy of IP_3-mediated Ca^{2+} signaling from global cellular oscillations to single-channel events. (A) Fluorescence traces illustrate global Ca^{2+} oscillations evoked by a strong (800-ms) UV photolysis flash in an SH-SY5Y cell loaded with fluo-4 and ciIP_3. (B) Local Ca^{2+} puffs evoked by weaker (100-ms flash) photorelease of i-IP_3 in another cell. (C) Image shows a Ca^{2+} puff (pseudocolored in green) captured at the time of peak amplitude from a single video frame and superimposed on a monochrome image of resting fluo-4 fluorescence in an SH-SY5Y cell. The trace shows a profile of Ca^{2+}-dependent fluorescence measured along the dotted line passing through the center of the puff. (D and E) Ca^{2+} puffs evoked, respectively, by strong and weak photolysis flashes equivalent to those in A and B after intracellular loading with EGTA. Global responses were abolished, and the traces show local signals measured from small regions of interest centered over puff sites. (F) Image shows a Ca^{2+} puff and corresponding fluorescence profile as in C, but recorded in the presence of EGTA. (G) Comparison of representative puffs recorded in SH-SY5Y cells after photorelease of iIP_3 using wide-field fluorescence microscopy (gray trace), and using TIRF microscopy together with EGTA loading (black trace). Both traces show fluorescence ratio changes ($\Delta F/F_0$) averaged within 1 × 1–μm regions of interest centered on puff sites. (H) Examples of sites that displayed exclusively single-channel blip activity. (I) Inset shows a Ca^{2+} signal from a 1-μm^2 region of interest, showing five discrete amplitude levels during a single puff. The histogram shows the distributions of event and step-level amplitudes derived from measurements at 87 sites in 20 cells, revealing "quantal" components at integer multiples of the single-channel level. A–F are adapted from Smith et al. (2009a), and G–I are from Smith and Parker (2009).

recordings of voltage- and ligand-gated Ca^{2+}-permeable channels expressed in the plasma membrane of *Xenopus* oocytes with a 2-ms temporal resolution and throughput of >500 simultaneous channels (Demuro and Parker, 2004, 2006). We initially assumed that the intracellular location of IP_3Rs would preclude their study using this approach because the puff sites in the oocyte are located a few μm inward from the membrane (Callamaras and Parker, 1999). However, we subsequently found that cultured human neuroblastoma SH-SY5Y cells and other mammalian cell lines possess puff sites that are located sufficiently close to the plasma membrane to be visualized by TIRF microscopy (Smith and Parker, 2009; Smith et al., 2009a).

A remaining problem was then how to achieve good control of cytosolic [IP_3]. Several studies in HeLa and other cultured cell lines had used extracellular agonists (Bootman et al., 1997a,b; Tovey et al., 2001) or membrane-permeant IP_3 (Thomas et al., 2000) to evoke Ca^{2+} events, but it was problematic to adjust the stimulus intensity to evoke puffs without triggering global Ca^{2+} waves. The injection of caged IP_3 into oocytes allows precise regulation of evoked Ca^{2+} signals through adjustment of the intensity and duration of UV photolysis flashes (Yao et al., 1995). But although caged IP_3 can be introduced into small cells via whole cell patch clamping (Stutzmann et al., 2003, 2004, 2006), this method is technically demanding and laborious. The recent commercial availability of a membrane-permeant ester of caged IP_3 (ciIP_3AM; SiChem) thus represented an important advance, facilitating precise control over $[IP_3]_i$, as illustrated in Fig. 1, where a strong UV flash evoked a global Ca^{2+} signal (Fig. 1 A), whereas a weaker flash (Fig. 1 B) evoked transient localized puffs. Nevertheless, the window of flash strengths over which discrete puffs were evoked was narrow, and puffs showed a wide spatial spread (Fig. 1 C). To mitigate these effects, we

further loaded cells by incubation with a membrane-permeant form of the slow Ca^{2+} buffer EGTA (Smith et al., 2009a) to "balkanize" global waves into local signals by disrupting CICR between puff sites (Callamaras and Parker, 2000; Dargan and Parker, 2003) and to sharpen the spatial and temporal profiles of puffs (Smith et al., 2009a; Zeller et al., 2009). This is illustrated in Fig. 1 D, where a global Ca^{2+} signal previously evoked by a strong UV flash devolved into discrete transients at individual puff sites.

The combination of TIRF imaging and cytosolic Ca^{2+} buffering by EGTA accomplished a dramatic improvement in the resolution of elementary and fundamental Ca^{2+} signals. Puffs imaged by wide-field microscopy show smoothly rising and falling phases on which it is not possible to resolve the step-wise changes that would be expected to arise from the openings and closings of individual IP_3R channels (Fig. 1 G, gray trace). However, in cells loaded with EGTA and visualized by TIRF microscopy, abrupt transitions in fluorescence levels are apparent on the falling (and sometimes rising) phase of the Ca^{2+} transient (Fig. 1 G, black trace). Several further observations support the interpretation that these steps arise from the openings and closings of individual IP_3R during a puff (Smith and Parker, 2009). (a) In addition to the puffs, sites often show smaller blips, with unitary fluorescence amplitudes. (b) Other sites, likely representing "lone" IP_3R channels, show only blips, giving fluorescence records that closely resemble single-channel patch clamp recordings (Fig. 1 H). (c) The durations of blips are exponentially distributed, with a mean closely matching the mean open time of IP_3R channels as measured by patch clamp (Smith and Parker, 2009). (d) A quantal analysis (Del Castillo and Katz, 1954) of step-wise fluorescence amplitude levels during puffs reveals a multimodal distribution, with recurring peaks at integer levels of the unitary blip amplitude (Fig. 1 I).

Quantal dissection of single-channel events underlying puffs. The ability to image puffs with single-channel resolution now allows us to dissect the quantal contributions of Ca^{2+} flux through individual IP_3Rs. By counting unitary steps, or by simply dividing the peak fluorescence of a Ca^{2+} puff by that of the unitary blip, one can determine the minimum number of functional IP_3Rs at a site. Our results indicate that puffs typically involve simultaneous opening of five to six IP_3Rs, although there is considerable heterogeneity between sites, with some containing >20 active IP_3Rs (Smith and Parker, 2009). Further, kinetic resolution of channel openings and closings during a puff allows the investigation of puff initiation and termination mechanisms. The rapid upstroke of puffs reflects a fast recruitment of IP_3Rs, with an opening rate of 1 channel ms^{-1} during the first 10 ms, decreasing abruptly to a rate 40 times lower within 20 ms. This rapid coordination likely arises because the high local Ca^{2+} resulting from the stochastic opening of an initial "trigger" channel evokes CICR from neighboring channels at the puff site. The mechanisms of puff termination still remain unclear, but we can rule out stochastic attrition (failure of CICR because all channels happen to randomly close at the same time) as the sole explanation as, contrary to observations, this predicts that puff durations would increase as an extremely steep function of the number of open channels. Further, depletion of luminal Ca^{2+} in the ER is unlikely to account for puff termination, as the step-wise decay of puffs continues at integer quantal levels. Instead, the

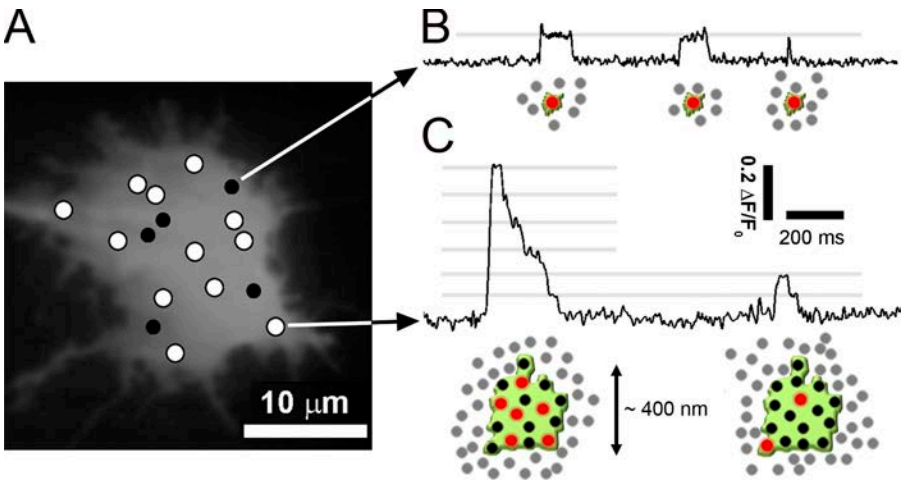

Figure 2. Schematic portrayal of the proposed arrangement of IP_3Rs underlying the generation of blips and puffs. (A) Monochrome image of resting fluo-4 fluorescence in an SH-SY5Y cell observed using TIRF microscopy, mapping sites that displayed single-channel blip activity in response to photoreleased IP_3 (black filled circles) and sites that displayed puffs (white circles). (B) The trace shows experimental data of activity recorded from a blip site. Cartoons illustrate our suggested arrangement and activity of IP_3R channels corresponding to each of the three blips during the trace. Channels open during each blip are shown in red, and closed channels are shown in black. Both are sensitized to IP_3 by binding to an as yet unidentified anchoring site (depicted in green). Motile, functionally unresponsive IP_3Rs are shown in gray. (C) Corresponding trace and cartoons illustrate the localization and activity of IP_3R channels during puffs. Gray lines indicate fluorescence levels corresponding to integer multiples of the single-channel (blip) level. The first puff (left) involves simultaneous opening of six channels at its peak, and the second puff (right) only two channels. The channels contributing to puffs are believed to be distributed across clusters with a diameter of roughly 400 nm.

progressive closure of IP_3R channels after the peak of a puff, with relatively few subsequent openings, is consistent with the rapid onset of a strong inhibitory process, likely resulting from the Ca^{2+}-dependent inhibition exhibited by the type 1 IP_3R predominant in SH-SY5Y cells (Smith and Parker, 2009).

Localization and motility–or immotility–of IP_3R channels. Optical single-channel imaging not only enables channel gating to be monitored, but also permits channel locations to be mapped with nano-scale precision, something that is not possible by patch clamp recording (Demuro and Parker, 2005; Smith et al., 2009b). We have applied this capability to study the clustered organization of IP_3Rs that underlies the generation of puffs and, in particular, to investigate whether these clusters are stable entities or may dynamically organize in response to stimulation.

Observations in many cell lines and in *Xenopus* oocytes have demonstrated numerous puffs arising over many minutes at fixed locations within a cell, suggesting that IP_3R clusters are relatively stable entities (Thomas et al., 1998; Tovey et al., 2001; Dargan and Parker, 2003; Smith et al., 2009a). By imaging blip sites we have found that lone IP_3R channels (blip sites) are similarly immotile within the ER membrane (Smith et al., 2009b; Wiltgen et al., 2010). These results present a paradox, as imaging studies using GFP-tagged or immunostained IP_3Rs have shown that a substantial proportion of IP_3Rs can diffuse freely within the ER membrane (Wilson et al., 1998; Fukatsu et al., 2004; Cruttwell et al., 2005; Ferreri-Jacobia et al., 2005; Iwai et al., 2005; Tateishi et al., 2005; Chalmers et al., 2006; Gibson and Ehrlich, 2008; Tojyo et al., 2008), and that they aggregate into clusters after sustained (minutes) activation of IP_3 signaling and/or cytosolic Ca^{2+} elevation (Wilson et al., 1998; Iwai et al., 2005; Tateishi et al., 2005; Chalmers et al., 2006; Tojyo et al., 2008; Taufiq-Ur-Rahman et al., 2009), or even undergo clustering in response to IP_3 within just a few seconds (Taufiq-Ur-Rahman et al., 2009). Moreover, there is a marked disparity between immunostaining patterns that show IP_3Rs distributed densely throughout the entirety of the cytoplasm (Wilson et al., 1998; Tateishi et al., 2005; Chalmers et al., 2006) versus Ca^{2+} release at just a few discrete puff and blip sites in mammalian cells (Fig. 2 A) (Bootman et al., 1997a,b; Thomas et al., 1998; Tovey et al., 2001; Smith and Parker, 2009; Smith et al., 2009a,b). As illustrated schematically in Fig. 2, we speculate that the difference may lie in the fact that different experimental approaches monitor different populations of IP_3Rs. Specifically, we propose that a majority of IP_3Rs (represented by gray dots in Fig. 2) may be motile but are either functionally unresponsive or mediate Ca^{2+} liberation only during sustained global elevations of cytosolic [Ca^{2+}] (Smith et al., 2009b). Local Ca^{2+} signals arise, instead, from a smaller subset of IP_3Rs that are anchored, individually or in clusters, by association with static cytoskeletal structures (represented in green) and which, possibly as a consequence of this anchoring, display high sensitivity to IP_3 to generate Ca^{2+} blips (Fig. 2 B) and puffs (Fig. 2 C).

Summary

Optical single-channel recording is a novel tool for the study of individual Ca^{2+}-permeable channels within intact cells under minimally perturbed physiological conditions. As applied to the functioning and spatial organization of IP_3Rs, this approach complements our existing knowledge, which derives largely from reduced systems—such as reconstitution into lipid bilayers and patch clamping of IP_3Rs on the membrane of excised nuclei—where the spatial arrangement and interactions among IP_3Rs via CICR are disrupted. The ability to image the activity of single IP_3R channels with millisecond resolution together with localization of their positions with a precision of a few tens of nanometers both raises several intriguing questions and holds promise of answers. In particular, what mechanism underlies the anchoring of puffs and blips to static locations; why do these Ca^{2+} release events appear to involve only a very small fraction of the IP_3Rs within a cell; and how can we reconcile the relative immotility of functional IP_3Rs with numerous studies reporting free diffusion of IP_3R protein in the ER membrane?

This Perspectives series includes articles by Gordon, Xie et al., Prosser et al., Santana and Navedo, and Hill-Eubanks et al.

REFERENCES

Axelrod, D. 2003. Total internal reflection fluorescence microscopy in cell biology. *Methods Enzymol.* 361:1–33. doi:10.1016/S0076-6879(03)61003-7

Berridge, M.J. 1997. Elementary and global aspects of calcium signalling. *J. Physiol.* 499:291–306.

Berridge, M.J., P. Lipp, and M.D. Bootman. 2000. The versatility and universality of calcium signalling. *Nat. Rev. Mol. Cell Biol.* 1:11–21. doi:10.1038/35036035

Bezprozvanny, I., J. Watras, and B.E. Ehrlich. 1991. Bell-shaped calcium-response curves of Ins(1,4,5)P_3- and calcium-gated channels from endoplasmic reticulum of cerebellum. *Nature.* 351:751–754. doi:10.1038/351751a0

Bootman, M.D., M.J. Berridge, and P. Lipp. 1997a. Cooking with calcium: the recipes for composing global signals from elementary events. *Cell.* 91:367–373. doi:10.1016/S0092-8674(00)80420-1

Bootman, M.D., E. Niggli, M. Berridge, and P. Lipp. 1997b. Imaging the hierarchical Ca^{2+} signalling system in HeLa cells. *J. Physiol.* 499:307–314.

Bootman, M.D., P. Lipp, and M.J. Berridge. 2001. The organisation and functions of local Ca^{2+} signals. *J. Cell Sci.* 114:2213–2222.

Callamaras, N., and I. Parker. 1999. Radial localization of inositol 1,4,5-trisphosphate–sensitive Ca^{2+} release sites in *Xenopus* oocytes resolved by axial confocal linescan imaging. *J. Gen. Physiol.* 113:199–213. doi:10.1085/jgp.113.2.199

Callamaras, N., and I. Parker. 2000. Phasic characteristic of elementary Ca^{2+} release sites underlies quantal responses to IP_3. *EMBO J.* 19:3608–3617. doi:10.1093/emboj/19.14.3608

Callamaras, N., J.S. Marchant, X.P. Sun, and I. Parker. 1998a. Activation and co-ordination of InsP_3-mediated elementary Ca^{2+} events during global Ca^{2+} signals in *Xenopus* oocytes. *J. Physiol.* 509:81–91. doi:10.1111/j.1469-7793.1998.081bo.x

Callamaras, N., X.P. Sun, I. Ivorra, and I. Parker. 1998b. Hemispheric asymmetry of macroscopic and elementary calcium signals mediated by InsP_3 in *Xenopus* oocytes. *J. Physiol.* 511:395–405. doi:10.1111/j.1469-7793.1998.395bh.x

Chalmers, M., M.J. Schell, and P. Thorn. 2006. Agonist-evoked inositol trisphosphate receptor (IP_3R) clustering is not dependent on changes in the structure of the endoplasmic reticulum. *Biochem. J.* 394:57–66. doi:10.1042/BJ20051130

Cheng, H., and W.J. Lederer. 2008. Calcium sparks. *Physiol. Rev.* 88:1491–1545. doi:10.1152/physrev.00030.2007

Cheng, H., W.J. Lederer, and M.B. Cannell. 1993. Calcium sparks: elementary events underlying excitation-contraction coupling in heart muscle. *Science.* 262:740–744. doi:10.1126/science.8235594

Cruttwell, C., J. Bernard, M. Hilly, V. Nicolas, R.E. Tunwell, and J.P. Mauger. 2005. Dynamics of the Ins(1,4,5)P_3 receptor during polarization of MDCK cells. *Biol. Cell.* 97:699–707. doi:10.1042/BC20040503

Dargan, S.L., and I. Parker. 2003. Buffer kinetics shape the spatiotemporal patterns of IP_3-evoked Ca^{2+} signals. *J. Physiol.* 553:775–788. doi:10.1113/jphysiol.2003.054247

Dargan, S.L., B. Schwaller, and I. Parker. 2004. Spatiotemporal patterning of IP_3-mediated Ca^{2+} signals in *Xenopus* oocytes by Ca^{2+}-binding proteins. *J. Physiol.* 556:447–461. doi:10.1113/jphysiol.2003.059204

Del Castillo, J., and B. Katz. 1954. Quantal components of the end-plate potential. *J. Physiol.* 124:560–573.

Demuro, A., and I. Parker. 2004. Imaging the activity and localization of single voltage-gated Ca^{2+} channels by total internal reflection fluorescence microscopy. *Biophys. J.* 86:3250–3259. doi:10.1016/S0006-3495(04)74373-8

Demuro, A., and I. Parker. 2005. "Optical patch-clamping": single-channel recording by imaging Ca^{2+} flux through individual muscle acetylcholine receptor channels. *J. Gen. Physiol.* 126:179–192. doi:10.1085/jgp.200509331

Demuro, A., and I. Parker. 2006. Imaging single-channel calcium microdomains. *Cell Calcium.* 40:413–422. doi:10.1016/j.ceca.2006.08.006

Demuro, A., and I. Parker. 2008. Multi-dimensional resolution of elementary Ca^{2+} signals by simultaneous multi-focal imaging. *Cell Calcium.* 43:367–374. doi:10.1016/j.ceca.2007.07.002

Dolmetsch, R.E., K. Xu, and R.S. Lewis. 1998. Calcium oscillations increase the efficiency and specificity of gene expression. *Nature.* 392:933–936. doi:10.1038/31960

Ehrlich, B.E., and J. Watras. 1988. Inositol 1,4,5-trisphosphate activates a channel from smooth muscle sarcoplasmic reticulum. *Nature.* 336:583–586. doi:10.1038/336583a0

Ferreri-Jacobia, M., D.O. Mak, and J.K. Foskett. 2005. Translational mobility of the type 3 inositol 1,4,5-trisphosphate receptor Ca^{2+} release channel in endoplasmic reticulum membrane. *J. Biol. Chem.* 280:3824–3831. doi:10.1074/jbc.M409462200

Foskett, J.K., C. White, K.H. Cheung, and D.O. Mak. 2007. Inositol trisphosphate receptor Ca^{2+} release channels. *Physiol. Rev.* 87:593–658. doi:10.1152/physrev.00035.2006

Fukatsu, K., H. Bannai, S. Zhang, H. Nakamura, T. Inoue, and K. Mikoshiba. 2004. Lateral diffusion of inositol 1,4,5-trisphosphate receptor type 1 is regulated by actin filaments and 4.1N in neuronal dendrites. *J. Biol. Chem.* 279:48976–48982. doi:10.1074/jbc.M408364200

Gee, K.R., K.A. Brown, W.N. Chen, J. Bishop-Stewart, D. Gray, and I. Johnson. 2000. Chemical and physiological characterization of fluo-4 Ca^{2+}-indicator dyes. *Cell Calcium.* 27:97–106. doi:10.1054/ceca.1999.0095

Gibson, C.J., and B.E. Ehrlich. 2008. Inositol 1,4,5-trisphosphate receptor movement is restricted by addition of elevated levels of O-linked sugar. *Cell Calcium.* 43:228–235. doi:10.1016/j.ceca.2007.05.008

Giepmans, B.N., S.R. Adams, M.H. Ellisman, and R.Y. Tsien. 2006. The fluorescent toolbox for assessing protein location and function. *Science.* 312:217–224. doi:10.1126/science.1124618

Grynkiewicz, G., M. Poenie, and R.Y. Tsien. 1985. A new generation of Ca^{2+} indicators with greatly improved fluorescence properties. *J. Biol. Chem.* 260:3440–3450.

Hamill, O.P., A. Marty, E. Neher, B. Sakmann, and F.J. Sigworth. 1981. Improved patch-clamp techniques for high-resolution current recording from cells and cell-free membrane patches. *Pflugers Arch.* 391:85–100. doi:10.1007/BF00656997

Hollingworth, S., J. Peet, W.K. Chandler, and S.M. Baylor. 2001. Calcium sparks in intact skeletal muscle fibers of the frog. *J. Gen. Physiol.* 118:653–678. doi:10.1085/jgp.118.6.653

Iwai, M., Y. Tateishi, M. Hattori, A. Mizutani, T. Nakamura, A. Futatsugi, T. Inoue, T. Furuichi, T. Michikawa, and K. Mikoshiba. 2005. Molecular cloning of mouse type 2 and type 3 inositol 1,4,5-trisphosphate receptors and identification of a novel type 2 receptor splice variant. *J. Biol. Chem.* 280:10305–10317. doi:10.1074/jbc.M413824200

Izu, L.T., W.G. Wier, and C.W. Balke. 1998. Theoretical analysis of the Ca^{2+} spark amplitude distribution. *Biophys. J.* 75:1144–1162. doi:10.1016/S0006-3495(98)74034-2

Kirber, M.T., E.F. Etter, K.A. Bellve, L.M. Lifshitz, R.A. Tuft, F.S. Fay, J.V. Walsh, and K.E. Fogarty. 2001. Relationship of Ca^{2+} sparks to STOCs studied with 2D and 3D imaging in feline oesophageal smooth muscle cells. *J. Physiol.* 531:315–327. doi:10.1111/j.1469-7793.2001.0315i.x

Lechleiter, J.D., S. Girard, E. Peralta, and D. Clapham. 1991. Spiral calcium wave propagation and annihilation in *Xenopus* laevis oocytes. *Science.* 252:123–126. doi:10.1126/science.2011747

Lechleiter, J.D., D.T. Lin, and I. Sieneart. 2002. Multi-photon laser scanning microscopy using an acoustic optical deflector. *Biophys. J.* 83:2292–2299. doi:10.1016/S0006-3495(02)73989-1

Lipp, P., and E. Niggli. 1996a. A hierarchical concept of cellular and subcellular Ca^{2+}-signalling. *Prog. Biophys. Mol. Biol.* 65:265–296. doi:10.1016/S0079-6107(96)00014-4

Lipp, P., and E. Niggli. 1996b. Submicroscopic calcium signals as fundamental events of excitation—contraction coupling in guinea-pig cardiac myocytes. *J. Physiol.* 492:31–38.

Mak, D.O., and J.K. Foskett. 1994. Single-channel inositol 1,4,5-trisphosphate receptor currents revealed by patch clamp of isolated *Xenopus* oocyte nuclei. *J. Biol. Chem.* 269:29375–29378.

Minta, A., J.P. Kao, and R.Y. Tsien. 1989. Fluorescent indicators for cytosolic calcium based on rhodamine and fluorescein chromophores. *J. Biol. Chem.* 264:8171–8178.

Navedo, M.F., G.C. Amberg, M. Nieves, J.D. Molkentin, and L.F. Santana. 2006. Mechanisms underlying heterogeneous Ca^{2+} sparklet activity in arterial smooth muscle. *J. Gen. Physiol.* 127:611–622. doi:10.1085/jgp.200609519

Neher, E. 1998. Vesicle pools and Ca^{2+} microdomains: new tools for understanding their roles in neurotransmitter release. *Neuron.* 20:389–399. doi:10.1016/S0896-6273(00)80983-6

Neher, E., and B. Sakmann. 1976. Single-channel currents recorded from membrane of denervated frog muscle fibres. *Nature.* 260:799–802. doi:10.1038/260799a0

Nguyen, Q.T., N. Callamaras, C. Hsieh, and I. Parker. 2001. Construction of a two-photon microscope for video-rate Ca^{2+} imaging. *Cell Calcium.* 30:383–393. doi:10.1054/ceca.2001.0246

Parker, I., and Y. Yao. 1991. Regenerative release of calcium from functionally discrete subcellular stores by inositol trisphosphate. *Proc Biol Sci.* 246:269–274. doi:10.1098/rspb.1991.0154

Parker, I., and Y. Yao. 1996. Ca^{2+} transients associated with openings of inositol trisphosphate-gated channels in *Xenopus* oocytes. *J. Physiol.* 491:663–668.

Parker, I., J. Choi, and Y. Yao. 1996. Elementary events of $InsP_3$-induced Ca^{2+} liberation in *Xenopus* oocytes: hot spots, puffs and blips. *Cell Calcium.* 20:105–121. doi:10.1016/S0143-4160(96)90100-1

Parys, J.B., S.W. Sernett, S. DeLisle, P.M. Snyder, M.J. Welsh, and K.P. Campbell. 1992. Isolation, characterization, and localization of the inositol 1,4,5-trisphosphate receptor protein in *Xenopus* laevis oocytes. *J. Biol. Chem.* 267:18776–18782.

Rose, H.J., S. Dargan, J. Shuai, and I. Parker. 2006. 'Trigger' events precede calcium puffs in *Xenopus* oocytes. *Biophys. J.* 91:4024–4032. doi:10.1529/biophysj.106.088872

Shuai, J., and I. Parker. 2005. Optical single-channel recording by imaging Ca^{2+} flux through individual ion channels: theoretical considerations and limits to resolution. *Cell Calcium.* 37:283–299. doi:10.1016/j.ceca.2004.10.008

Shuai, J., H.J. Rose, and I. Parker. 2006. The number and spatial distribution of IP_3 receptors underlying calcium puffs in *Xenopus* oocytes. *Biophys. J.* 91:4033–4044. doi:10.1529/biophysj.106.088880

Smith, I.F., and I. Parker. 2009. Imaging the quantal substructure of single IP_3R channel activity during Ca^{2+} puffs in intact mammalian cells. *Proc. Natl. Acad. Sci. USA.* 106:6404–6409. doi:10.1073/pnas.0810799106

Smith, I.F., S.M. Wiltgen, and I. Parker. 2009a. Localization of puff sites adjacent to the plasma membrane: functional and spatial characterization of Ca^{2+} signaling in SH-SY5Y cells utilizing membrane-permeant caged IP_3. *Cell Calcium.* 45:65–76. doi:10.1016/j.ceca.2008.06.001

Smith, I.F., S.M. Wiltgen, J. Shuai, and I. Parker. 2009b. Ca^{2+} puffs originate from preestablished stable clusters of inositol trisphosphate receptors. *Sci. Signal.* 2:ra77. doi:10.1126/scisignal.2000466

Stutzmann, G.E., F.M. LaFerla, and I. Parker. 2003. Ca^{2+} signaling in mouse cortical neurons studied by two-photon imaging and photoreleased inositol triphosphate. *J. Neurosci.* 23:758–765.

Stutzmann, G.E., A. Caccamo, F.M. LaFerla, and I. Parker. 2004. Dysregulated IP_3 signaling in cortical neurons of knock-in mice expressing an Alzheimer's-linked mutation in presenilin1 results in exaggerated Ca^{2+} signals and altered membrane excitability. *J. Neurosci.* 24:508–513. doi:10.1523/JNEUROSCI.4386-03.2004

Stutzmann, G.E., I. Smith, A. Caccamo, S. Oddo, F.M. Laferla, and I. Parker. 2006. Enhanced ryanodine receptor recruitment contributes to Ca^{2+} disruptions in young, adult, and aged Alzheimer's disease mice. *J. Neurosci.* 26:5180–5189. doi:10.1523/JNEUROSCI.0739-06.2006

Sun, X.P., N. Callamaras, J.S. Marchant, and I. Parker. 1998. A continuum of $InsP_3$-mediated elementary Ca^{2+} signalling events in *Xenopus* oocytes. *J. Physiol.* 509:67–80. doi:10.1111/j.1469-7793.1998.067bo.x

Tateishi, Y., M. Hattori, T. Nakayama, M. Iwai, H. Bannai, T. Nakamura, T. Michikawa, T. Inoue, and K. Mikoshiba. 2005. Cluster formation of inositol 1,4,5-trisphosphate receptor requires its transition to open state. *J. Biol. Chem.* 280:6816–6822. doi:10.1074/jbc.M405469200

Taufiq-Ur-Rahman, A. Skupin, M. Falcke, and C.W. Taylor. 2009. Clustering of $InsP_3$ receptors by $InsP_3$ retunes their regulation by $InsP_3$ and Ca^{2+}. *Nature.* 458:655–659. doi:10.1038/nature07763

Thomas, D., P. Lipp, M.J. Berridge, and M.D. Bootman. 1998. Hormone-evoked elementary Ca^{2+} signals are not stereotypic, but reflect activation of different size channel clusters and variable recruitment of channels within a cluster. *J. Biol. Chem.* 273:27130–27136. doi:10.1074/jbc.273.42.27130

Thomas, D., P. Lipp, S.C. Tovey, M.J. Berridge, W. Li, R.Y. Tsien, and M.D. Bootman. 2000. Microscopic properties of elementary Ca^{2+} release sites in non-excitable cells. *Curr. Biol.* 10:8–15. doi:10.1016/S0960-9822(99)00258-4

Thorn, P., A.M. Lawrie, P.M. Smith, D.V. Gallacher, and O.H. Petersen. 1993. Local and global cytosolic Ca^{2+} oscillations in exocrine cells evoked by agonists and inositol trisphosphate. *Cell.* 74:661–668. doi:10.1016/0092-8674(93)90513-P

Tojyo, Y., T. Morita, A. Nezu, and A. Tanimura. 2008. The clustering of inositol 1,4,5-trisphosphate (IP_3) receptors is triggered by IP_3 binding and facilitated by depletion of the Ca^{2+} store. *J. Pharmacol. Sci.* 107:138–150. doi:10.1254/jphs.08021FP

Tovey, S.C., P. de Smet, P. Lipp, D. Thomas, K.W. Young, L. Missiaen, H. De Smedt, J.B. Parys, M.J. Berridge, J. Thuring, et al. 2001. Calcium puffs are generic $InsP_3$-activated elementary calcium signals and are downregulated by prolonged hormonal stimulation to inhibit cellular calcium responses. *J. Cell Sci.* 114:3979–3989.

Ventura, A.C., L. Bruno, A. Demuro, I. Parker, and S.P. Dawson. 2005. A model-independent algorithm to derive Ca^{2+} fluxes underlying local cytosolic Ca^{2+} transients. *Biophys. J.* 88:2403–2421. doi:10.1529/biophysj.104.045260

Wang, S.Q., L.S. Song, E.G. Lakatta, and H. Cheng. 2001. Ca^{2+} signalling between single L-type Ca^{2+} channels and ryanodine receptors in heart cells. *Nature.* 410:592–596. doi:10.1038/35069083

Wilson, B.S., J.R. Pfeiffer, A.J. Smith, J.M. Oliver, J.A. Oberdorf, and R.J. Wojcikiewicz. 1998. Calcium-dependent clustering of inositol 1,4,5-trisphosphate receptors. *Mol. Biol. Cell.* 9:1465–1478.

Wiltgen, S.M., I.F. Smith, and I. Parker. 2010. Super-resolution localization of single functional inositol trisphosphate receptors channels utilizing calcium flux as a readout. *Biophys. J.* In press.

Yao, Y., and I. Parker. 1994. Ca^{2+} influx modulation of temporal and spatial patterns of inositol trisphosphate-mediated Ca^{2+} liberation in *Xenopus* oocytes. *J. Physiol.* 476:17–28.

Yao, Y., J. Choi, and I. Parker. 1995. Quantal puffs of intracellular Ca^{2+} evoked by inositol trisphosphate in *Xenopus* oocytes. *J. Physiol.* 482:533–553.

Zeller, S., S. Rüdiger, H. Engel, J. Sneyd, G. Warnecke, I. Parker, and M. Falcke. 2009. Modeling of the modulation by buffers of Ca^{2+} release through clusters of IP_3 receptors. *Biophys. J.* 97:992–1002. doi:10.1016/j.bpj.2009.05.050

Zou, H., L.M. Lifshitz, R.A. Tuft, K.E. Fogarty, and J.J. Singer. 2004. Using total fluorescence increase (signal mass) to determine the Ca^{2+} current underlying localized Ca^{2+} events. *J. Gen. Physiol.* 124:259–272. doi:10.1085/jgp.200409066